



Differences in moisture sorption characteristics and browning of lesser mealworm (*Alphitobius diaperinus*) ingredients

He Sun^a, Ornella Necochea Velazco^a, Catriona Lakemond^a, Matthijs Dekker^a, Lee Cadesky^b, Maryia Mishyna^{a,*}

^a Food Quality & Design Group, Wageningen University & Research, 6700 AA, Wageningen, the Netherlands

^b Protifarm Processing B.V., Harderwijkerweg 141B, 3852 AB, Ermelo, the Netherlands

ARTICLE INFO

Keywords:

Browning
Lesser mealworm
Modelling
Proteins
Sorption isotherms

ABSTRACT

Lesser mealworm (*Alphitobius diaperinus*) is an insect species that can be reared on an industrial scale for human consumption. In this study, the hydration behavior of processed lesser mealworm food ingredients (whole powder, protein concentrate, textured protein) was analyzed in comparison to whey protein concentrate and tofu. Moisture adsorption isotherms were determined gravimetrically over 0.11–0.96 water activity range at 5 and 20 °C, and seven sorption models were applied to fit the experimental data. The Guggenheim-Anderson-de Boer model performed best on the isotherms of all studied samples. The determined adsorption isotherms were type III according to Brunauer classification. Mealworm protein concentrate presented the strongest hydration capacity at 20 °C, followed by whey protein concentrate and whole mealworm powder. Textured mealworm protein and tofu exhibited similar hydration behavior at 5 °C. Moreover, browning and agglomeration of mealworm protein concentrate powder were observed at water activities of 0.73 and higher, which can be explained by its composition and porous structure and were not typical for whey protein concentrate. The moisture adsorption results are important for the prediction of lesser mealworm ingredients shelf-life or prevention of undesirable quality changes during storage, but more research on microbial growth and sensory quality is needed.

1. Introduction

The world population is expected to increase to 9.7 billion in 2050 (United Nations, 2019), this comes with an increasing demand for animal protein, limited land area, and low sustainability of existing food production systems. In this regard, the studies for new protein sources are emerging over recent years (Fasolin et al., 2019). Edible insects are drawing more attention and are considered as an alternative to conventional meat products due to their nutritional value and sustainability of production, leading to less greenhouse gas emissions and reduced land and water usage (van Huis, & Tomberlin, 2017). Although insects have been used as traditional foods in some tropical countries (DeFoliart, 1992), their consumption is still not fully accepted by many western societies due to people's natural negative attitude towards them. So far, many efforts have been made to promote the edible insect market and to increase acceptance (Shockley, Allen, & Gracer, 2017). One successful strategy is processing insects into powder, protein

isolates, and oils that can be used in the formulation of novel insect-based foods in order to attract consumers. This has been successfully demonstrated in the lesser mealworm (*Alphitobius diaperinus*) of which food ingredients products are available in Western Europe. Regarding proteins, the lesser mealworm has high protein content and its essential amino acid content is comparable to soybean proteins (Yi et al., 2013).

Water content and its interaction with food components usually determines the stability of a food system (Rahman, 2010). Moisture sorption reflects the relationship between moisture content and water activity at given temperature and pressure. It plays an important role in physicochemical and biological changes of food products (e.g., browning, lipid oxidation, and microbial growth (Caballero-Cerón, Guerrero-Beltrán, Mújica-Paz, Torres, & Welti-Chanes, 2015)). Various types of food products often exhibit different properties. For instance, powder products tend to absorb water and form agglomerates especially in humid conditions, which could impair not only the functional

* Corresponding author.

E-mail address: maryia.mishyna@wur.nl (M. Mishyna).

<https://doi.org/10.1016/j.lwt.2021.110989>

Received 21 July 2020; Received in revised form 24 January 2021; Accepted 25 January 2021

Available online 29 January 2021

0023-6438/© 2021 The Author(s). Published by Elsevier Ltd. This is an open access article under the CC BY license (<http://creativecommons.org/licenses/by/4.0/>).

properties but also lower the quality of final products (Aguilera, del Valle, & Karel, 1995). Different forces and the intermolecular structure of food components are involved in the agglomeration phenomenon (Zafar, Vivacqua, Calvert, Ghadiri, & Cleaver, 2017). Therefore, understanding the characteristics of food ingredients and their moisture sorption properties is a prerequisite for package selection and better preservation. It is also essential for product design, process optimization, and for further understanding of the sorption mechanisms in food products (Al-Muhtaseb, McMinn, & Magee, 2002).

There are numerous studies on the moisture sorption behavior of conventional food systems under different conditions. For instance, it has been shown that increasing temperature decreased the equilibrium moisture content of fish meal (Vivanco & Taboada, 1998). Singh et al. reported that type II desorption isotherms of smoked chicken sausages were best fitted with Halsey equation and pore size increased when rising temperatures (Singh, Rao, Anjaneyulu, & Patil, 2001), while Sawhney et al. also determined type II sorption isotherms for whey protein concentrate, but the isotherms were best fitted with GAB equation at 25, 35, and 45 °C (Sawhney, Sarkar, Patil, & Sharma, 2014). Tham et al. observed lactose crystallization in three infant formulas at 0.428 water activity and caking in water activity range of 0.330–0.753 (Tham, Wang, Yeoh, & Zhou, 2016). However, the relevant studies for edible insects are limited. One of few available studies on insects demonstrated that cricket powder had higher hydration capacity than black soldier fly larvae, attributing to compositional and physicochemical differences and affecting its shelf-life (Kamau et al., 2018). Azzollini et al. found that blanching treatment reduced the hygroscopicity of yellow mealworm powder and GAB model well described its hydration behavior (Azzollini, Derossi, & Severini, 2016). However, to the best of our knowledge, the hydration behavior of processed lesser mealworm has not been studied yet, but it is important to get insight for preventing the occurrence of undesirable reactions and ensuring the stability of insect ingredients during storage.

Therefore, this study aimed to obtain moisture adsorption isotherms of lesser mealworm ingredients and to determine a suitable model describing these isotherms. Isotherms of lesser mealworm powder (IP), lesser mealworm protein concentrate (IPC), and whey protein concentrate (WPC) were studied at 20 °C and isotherms of IP, textured lesser mealworm protein (TIP) and tofu - at 5 °C. WPC and tofu were included for comparison to lesser mealworm ingredients. Additionally, powder agglomeration and color characteristics of IPC and WPC as a function of water activities were investigated.

2. Materials and methods

2.1. Materials

Lesser mealworm (*Alphitobius diaperinus*) products IP, IPC, and TIP were supplied by Protifarm (Ermelo, the Netherlands). IP represented 100% whole powder obtained from blanched, dried, and grinded lesser mealworms. IPC is high protein processed powder and TIP is coagulated protein product from lesser mealworm. All products were produced in accordance with HACCP guidelines. WPC was purchased from Bulk-powders (Colchester, England), tofu - from Jumbo supermarket (Wageningen, the Netherlands). The salts used were reagent grade and purchased from Sigma-Aldrich (the Netherlands). Thymol (2-isopropyl-5-methylphenol, ≥98.5%) was purchased from Sigma-Aldrich (the Netherlands), petroleum ether 40–60 °C (PEC grade) - from Actua-All Chemicals (the Netherlands).

2.2. Proximate composition analysis

The content of dry matter, crude protein, crude fat, and ash were measured for IP, IPC, TIP, WPC, and tofu (Fig. S1) according to AOAC (Horwitz, 1975). Different nitrogen-to-protein conversion factors (Kp) were used to calculate protein content. A Kp of 4.76 was used for whole

insect powder (Janssen, Vincken, Van Den Broek, Fogliano, & Lake-mond, 2017), a Kp of 5.60 - for insect protein concentrate and textured insect protein (Janssen et al., 2017), and a Kp of 6.25 - for WPC and tofu (Khatib, Aramouni, Herald, & Boyer, 2002; Rouch, Roupas, & Roginski, 2007). The content of carbohydrate was calculated by subtracting the contents of protein, fat, and ash from 100%. Each measurement was performed in triplicate.

2.3. Particle size distribution

The particle size distribution of three powder products (IP, IPC, and WPC) was determined via sieve classification with some modifications (Strange & Onwulata, 2002). Test sieves with pore sizes of 1.250, 1.000, 0.425, 0.315, and 0.180 mm and FRITSCH sieve shaker (Germany) were used. The particle size distribution was presented as a mass fraction on a dry basis.

2.4. Surface morphology

The surface morphology of IP, IPC, TIP, WPC, and tofu was measured by Magellan 400 scanning electron microscopy (United States). Critical point drying method was used to dehydrate tofu, the other samples were dried in an oven at 31 °C under vacuum for 48 h. All samples were then coated with 12 nm of tungsten and analyzed in the scanning electron microscopy with a beam current of 13 pA, 2.00 kV. The magnification of images was from 250× to 10000×.

2.5. Color analysis

The color of IPC and WPC was measured by Hunterlab color flex (Virginia, United States). The total color difference (ΔE) of equilibrated samples at each water activity was compared with the initial ones after the first drying. Browning index (BI) defined as the purity of brown color is frequently used as an indicator of enzymatic or nonenzymatic browning (Buera, Lozano, & Petriella, 1986; Guerrero, Alzamora, & Gerschenson, 1996) and was determined according to (Lenaerts, Van Der Borght, Callens, & Van Campenhout, 2018; Palou, Lopez-Malo, Barbosa-Canovas, Welte-Chanes, & Swanson, 1999).

Iris V 400 (Instrument Solutions Benelux, France) was used to take the picture and analyze the color of IPC and WPC. The method type was single snapshot, the lens was a Balser 25 mm, the light mode was top and bottom light. Image size was selected as the default settings (width = 2588, height = 1942, X axis = 0, Y axis = 0). Principal component analysis (PCA) was used to visualize the differences in color among the samples. The threshold value of color spectrum was set at 1%.

2.6. Water activity measurements

Novasina LabMaster-aw (Lachen, Switzerland) was used to measure the water activities of IP, IPC, TIP, WPC, and tofu before the experiment, as well as the water activities of studied samples during moisture adsorption experiment. The temperature was set at 25 °C. The stable observation time of a chamber was 1 min (Aw) and 2 min (temperature). The measurements were performed in quadruplicate.

2.7. Moisture adsorption isotherms

As the storage recommended temperatures vary for products with different water activities, the adsorption isotherms were determined at 20 °C for IP, IPC, WPC, and at 5 °C for TIP and tofu. The isotherm of IP at 5 °C was also determined to study the temperature effect. Isotherms were obtained by static gravimetric method (Caballero-Cerón, Guerrero-Beltrán, Mújica-Paz, Torres, & Welte-Chanes, 2015). Nine saturated salt solutions (LiCl, CH₃COOK, MgCl₂, K₂CO₃, Mg(NO₃)₂, NaCl, SrCl₂, KCl, KNO₃) with a water activity range of 0.11–0.96 were used (Greenspan, 1977; Kiranoudis, Maroulis, Tsami, & Marinou-Kouris,

1993). The water activity of saturated salt solutions at different temperatures (Caballero-Cerón et al., 2015; Greenspan, 1977; López-Malo, Palou, & Argai, 1994) and the specifications of preparing saturated salt solutions are presented in Table S1. Salt solutions with the excess salt were stirred once a day for five days to assure the right formation of the saturated solution and then transferred into desiccators two days before the experiment.

An amount of 1.00 ± 0.01 g sample was weighed into pre-weighed aluminium plates (W_1) and dried at 55°C for 24 h that was determined sufficient by preliminary tests. The weight of sample and plate was recorded (W_2) after drying. Each desiccator contained 4 dried samples. Crystalline thymol was placed inside the desiccators with $A_w > 0.60$ to inhibit microbial growth. To ensure the accuracy, one sample was taken as an indicator for each desiccator. The weight and A_w of the indicator was measured after every 2 days until the difference in weight between two consecutive measurements was about ± 0.001 g representing that samples were at the equilibrium state. Then the measurements for the other samples were performed. Considering the atmospheric effect on sample during weighing, the operation was done as quickly as possible, generally within 30 s (Kiranoudis et al., 1993). The weight of equilibrated sample and plate was recorded (W_3). The equilibrium moisture content (EMC) (g/100 g dry basis) was calculated by the following formula:

$$\text{Equilibrium moisture content (EMC)} = \frac{W_3 - W_2}{W_2 - W_1} * 100. \quad (1)$$

The isotherm was made by plotting EMC against corresponding water activities. For each isotherm, 27 experimental data points were used to create the plot.

Water binding capacity (WBC) related to high moisture systems (Chen, Piva, & Labuza, 1984; Wallingford & Labuza, 1983) was determined to compare the capacity of different types of products to bind water. WBC data were taken as the EMC values at the $A_w = 0.95$ (20°C) and $A_w = 0.96$ (5°C), respectively (Chen et al., 1984; Wallingford & Labuza, 1983).

2.8. Mathematical modelling of sorption isotherms

Experimental data were fitted to 7 sorption models Brunauer-Emmett-Teller (BET), Guggenheim-Anderson-de Boer (GAB), Kuhn, Smith, Caurie, Halsey, and Oswin that were frequently applied (Al-Muhtaseb et al., 2002; Caballero-Cerón et al., 2015; Caurie, 1981; Kamau et al., 2018; Smith, 1947). The mathematical equations of each model and the corresponding range of water activity are presented in Table S2. The model parameters were estimated by non-linear regression to minimize the residual sums of squares using SolverAid, Microsoft Excel 365 ProPlus software (Salter & De Levie, 2002). Akaike information criterion (AIC) was used to compare different models and evaluate the goodness of fit of each model. Due to a small number of experiments, a corrected version (AIC_c) was used by the equation below (Burnham & Anderson, 2002):

$$AIC_c = n * \ln(S^2) + 2 * (p + 1) * \frac{n}{n - p} \quad (2)$$

where n is the number of data points, $S^2 = SS_{\text{res}}/n$ with SS_{res} the residual sums of squares, p is the number of model parameters. The term AIC differences (ΔAIC_c) was used to interpret the quality of model. The equation of ΔAIC_c was listed below (Burnham & Anderson, 2002):

$$AIC_c = AIC_{ci} - AIC_{\min} \quad (3)$$

where AIC_{ci} is the AIC_c value of each model, AIC_{\min} is the minimum value of all. The model with the minimum AIC_c indicates the best one. Models with $0 < \Delta AIC_c < 4$ have substantial support to be considered as a good model (Burnham & Anderson, 2002). In addition, residuals plot was used to evaluate the quality of the model. A random and

homoscedastic residual distribution indicates a good fit of data.

2.9. Data analysis

The significance test ($\alpha = 0.05$) was performed via LSD and Tukey post hoc test in IBM SPSS statistics 22. In the case of small number of samples, Shapiro-Wilk test ($\alpha = 0.05$) was applied to check the normality distribution of moisture adsorption data. The extended uncertainties (U) of EMC at each water activity were calculated by the following formula (Bell, 2001; Bui, Labat, & Aubert, 2017):

$$U = k * \sqrt{u_A^2 + u_B^2} \quad (4)$$

where u_A represents random uncertainty (Type A uncertainty), u_B represents systematic uncertainty (Type B uncertainty). Assuming that the results were normally distributed, and coverage factor $k = 2$ to give a level of confidence of approximately 95%. u_A was calculated by the following formula (Bell, 2001; Bui et al., 2017):

$$u_A = \frac{s}{\sqrt{n}} \quad (5)$$

where s is the standard deviation, n is the number of measurements. As the EMC value was calculated by Equation (4), so the systematic uncertainty of EMC includes the uncertainties of 3 different mass measurements (W_3 , W_2 , and W_1) and the uncertainty of dry matter content measurements (d). u_B was calculated by summing the partial derivatives of each parameter (Bell, 2001; Bui et al., 2017):

$$u_B = \sqrt{\sum_i \left(\frac{\partial W}{\partial x_i} * u(x_i) \right)^2} \quad (6)$$

The same gravimetric scale (METTLER TOLEDO AE200, United States) was used to measure W_3 , W_2 , and W_1 for the whole experiments. Applying Equations (1) and (6) to this case leads to:

$$u_B = \sqrt{\left[\frac{2}{W_1^2 * d^2} + \left(\frac{W_2 - W_3}{W_1^2 * d} \right)^2 \right] * u_B(W)^2 + \left(\frac{W_2 - W_3}{W_1 * d^2} \right)^2 * u_B(d)^2} \quad (7)$$

$u_B(W)$ represents the uncertainty of the scale which was calculated by the following formula (Bui et al., 2017):

$$u_B(W)^2 = \left(\frac{u_{\text{Disp}}}{\sqrt{3}} \right)^2 + \left(\frac{u_{\text{Lin}}}{\sqrt{3}} \right)^2 \quad (8)$$

where u_{Disp} (display resolution) and u_{Lin} (linearity) are 0.0001 and 0.0003, respectively, found in the instruction of scale.

3. Results and discussion

3.1. Proximate composition

The results of proximate composition and water activities (Table 1) shows that IP, IPC, and WPC were low moisture content products (95.5–98.7% dry matter content, $A_w = 0.146$ – 0.206), while TIP and tofu were high in moisture content (23.9–28.4% dry matter content, $A_w = 0.971$ – 0.972). The proximate composition of IP was comparable to the composition of lesser mealworm powder (58.4% protein, 26.3% fat, and 5.4% ash) previously described (Janssen et al., 2017). As the nutrients of larvae are affected by diets and development state (van Broekhoven, Oonincx, van Huis, & van Loon, 2015), there might be variations in its composition between studies. As shown in Table 1, IPC has a higher content of fat (16.8%) and carbohydrate (23.8%), but lower protein content (53.9%) in comparison to WPC (1.0% fat, 16.7% carbohydrate, and 78.5% protein). Similarly, higher fat and carbohydrate content, but lower protein content were also found in TIP compared to tofu. Although IPC and TIP were expected to be similar to WPC and tofu in terms of

Table 1

Proximate composition and water activity of IP, IPC, TIP, WPC, and tofu.

	IP	IPC	TIP	WPC	Tofu
Composition, %					
dry matter ¹	98.7 ± 0.0 ^{a,2}	96.7 ± 0.1 ^b	28.4 ± 0.5 ^d	95.5 ± 0.2 ^c	23.9 ± 0.4 ^e
protein	46.7 ± 0.5 ^c	53.9 ± 0.2 ^{bc}	47.9 ± 3.2 ^c	78.5 ± 0.2 ^a	59.4 ± 7.3 ^b
fat	27.9 ± 0.2 ^a	16.8 ± 0.9 ^b	8.3 ± 0.7 ^c	1.0 ± 0.1 ^e	5.0 ± 0.2 ^d
ash	3.5 ± 0.0 ^c	5.5 ± 0.0 ^a	3.0 ± 0.1 ^d	3.9 ± 0.0 ^b	5.5 ± 0.0 ^a
Carbohydrate ³	21.8 ± 0.7 ^{bc}	23.8 ± 1.0 ^{bc}	40.8 ± 2.6 ^a	16.7 ± 0.1 ^d	30.1 ± 7.1 ^b
Aw	0.146 ± 0.006 ^{d,4}	0.206 ± 0.03 ^b	0.972 ± 0.001 ^a	0.189 ± 0.001 ^c	0.971 ± 0.001 ^a

¹ Dry matter content was determined on fresh basis, the other results were presented as g/100 g dry basis.

² Mean ± standard deviation, n = 3, the same superscript letters in the same row are not significantly different (p > 0.05).

³ The content of carbohydrate was calculated by subtracting the contents of protein, fat, and ash from 100%, ⁴Mean ± standard deviation, n = 4.

product type, respectively, they slightly differed in compositions. The higher carbohydrate content of these insect products is partly explained by the fact that insects contain amounts of chitin (Janssen et al., 2017).

3.2. Particle size distribution

The result of particle size distribution of three powder products (IP, IPC, and WPC) (Fig. 1) shows that IP and IPC particles were mostly distributed (76 and 70%, respectively) above 1.250 mm, which means both of them were made up of relatively large particles. While IPC contained much smaller sized particles (less than 0.425 mm) compared to IP (above 0.425 mm). In contrast, half of WPC consisted of small sized particles (0.180–0.315 mm) with the largest one being less than 1.000 mm. The difference in particle size of IPC and WPC can be partly explained by clumping of IPC powder which was observed during the movement of the sieve and shaking machine and higher fat content in IPC comparing to WPC.

3.3. Surface morphology

IP, IPC, TIP, WPC, and tofu were observed under scanning electron microscopy (SEM). IP was made up of large pieces of insect tissues with a few cracks (Figs. 2 and 1a), but no pores were observed on the outer surface (Figs. 2 and 1b). The surface of IPC had a porous microstructure with a large number of pores (Fig. 2 and a), while less porous surface structure was observed for WPC particles (Figs. 2 and 3a), suggesting

that IPC and WPC had different surface properties. The clumping of IPC powder was also observed on microphotographs, e.g., the spherical-shaped IPC particles aggregated with each other (Fig. 2 and b), resulting in large agglomerated particles. WPC particles presented a “cell” shape of different sizes and were relatively dispersed under SEM (Figs. 2 and 3b). TIP and tofu were similar in surface morphology (Figs. 2, 4a and 5a), both exhibited a few pores.

3.4. Analysis of color

Browning of IPC samples was observed at higher water activities (Aw > 0.73) after around 8 days, while the color of WPC samples did not change significantly. In particular, BI values of IPC over the water activity range of 0.73–0.95 (SrCl₂–KNO₃) were much higher than that of IPC at lower water activities (Fig. 3), that suggests that evident browning phenomenon occurred over this range. No significant differences in the BI values were found for WPC, indicating that no evident browning of WPC has occurred.

In Fig. 4, the samples in PC1 direction show the largest variation, and PC2 axis is the second most important direction which is orthogonal to PC1 (Kassambara, 2016). The data points of IPC at Aw ranging from 0.73 to 0.95 were grouped and separated from the other groups (Fig. 4a), i.e. the color of IPC samples over this water activity range (0.73–0.95) was significantly different from the others. It supports the observed browning in IPC at higher water activities (0.73–0.95). As for WPC, the overall distribution of data points was relatively close (Fig. 4b). Also, the samples after drying and with KNO₃ solution treatment were found similar in PC1 direction. This means no evident color change occurred in WPC. It can be also seen from Fig. 4a, that the texture of IPC had changed a lot. The particles of IPC at higher water activities (0.73–0.95) aggregated and texture of the one at Aw of 0.95 became more liquid like, while the others remained powder state. However, caking of WPC was observed only at Aw of 0.95 (Fig. 4b).

Azzollini et al. also observed color alternation in freeze-dried yellow mealworm larvae (Azzollini et al., 2016), assuming that the enzymatic browning as a result of hydration of enzymes caused the color change of the sample, while non-enzymatic browning could also occur due to the absorption of moisture. Labuza found that non-enzymatic browning began when monolayer moisture was formed, and reaction rates could increase to a maximum at Aw of 0.70 (Labuza, 1977). Therefore, non-enzymatic browning reaction likely explains the browning in this study, considering the inactivation of enzymes caused by heat treatment temperatures higher than 80 °C during the sample preparation. This idea is supported by the composition of IPC with protein and also a substantial carbohydrate content. In particular, the higher carbohydrate content of IPC compared to WPC could accelerate the process of browning and adsorption of water. The role of Maillard reaction in browning of IPC and the presence of reducing sugars in lesser mealworm

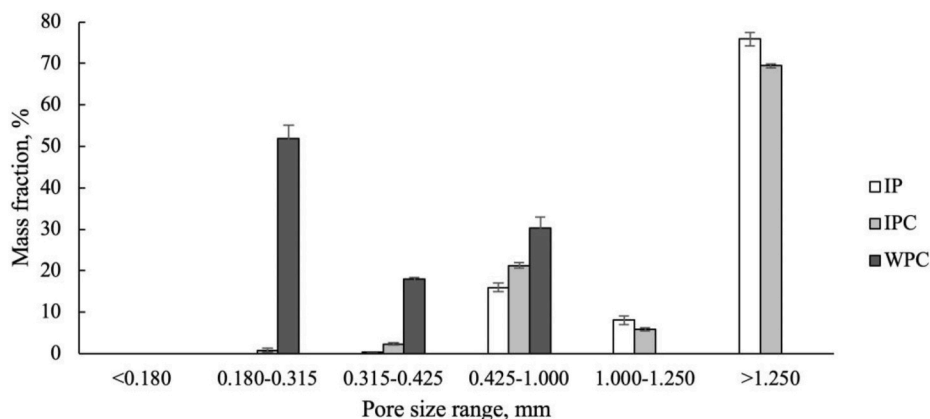


Fig. 1. Particle size distribution (mass fraction, %) of IP, IPC, and WPC.

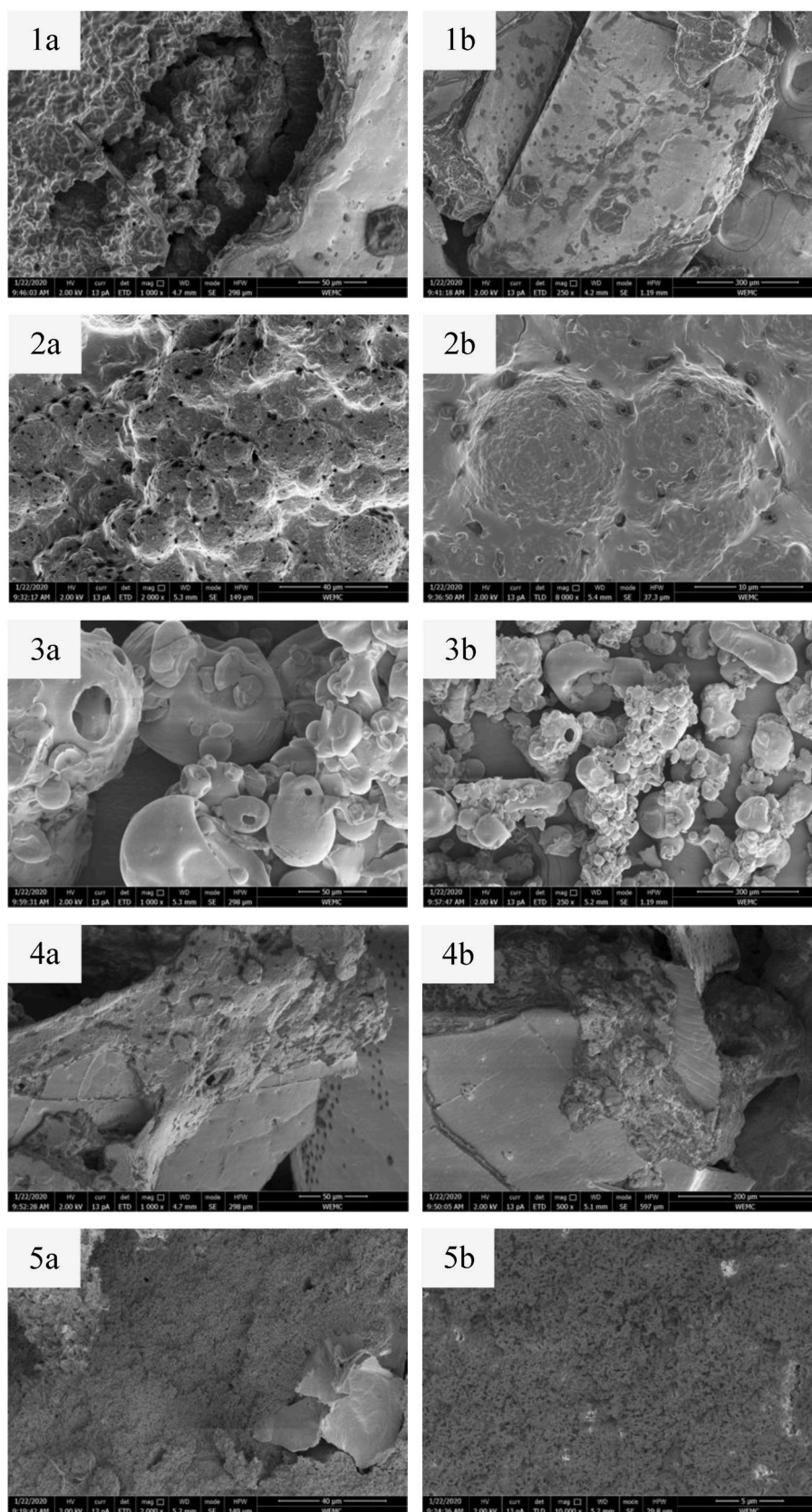


Fig. 2. Scanning electron microscopy (SEM) photographs of IP (1a: 1000 \times , 1b: 250 \times), IPC (2a: 2000 \times , 2b: 8000 \times), WPC (3a: 1000 \times , 3b: 250 \times), TIP (4a: 1000 \times , 4b: 500 \times), and tofu (5a: 2000 \times , 5b: 10000 \times). All samples were dehydrated and coated with tungsten before the analysis.

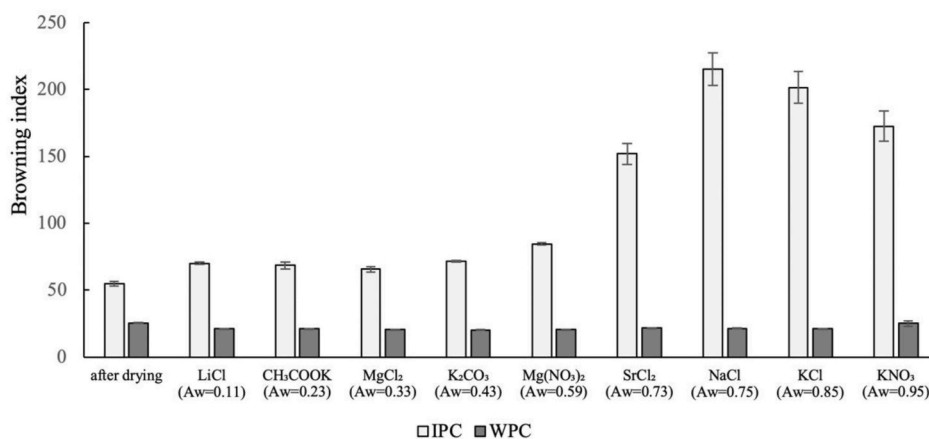


Fig. 3. Browning index of IPC and WPC after incubation for 8 days at 0.11–0.96 water activity (A_w) range at 20 °C measured with Iris V 400.

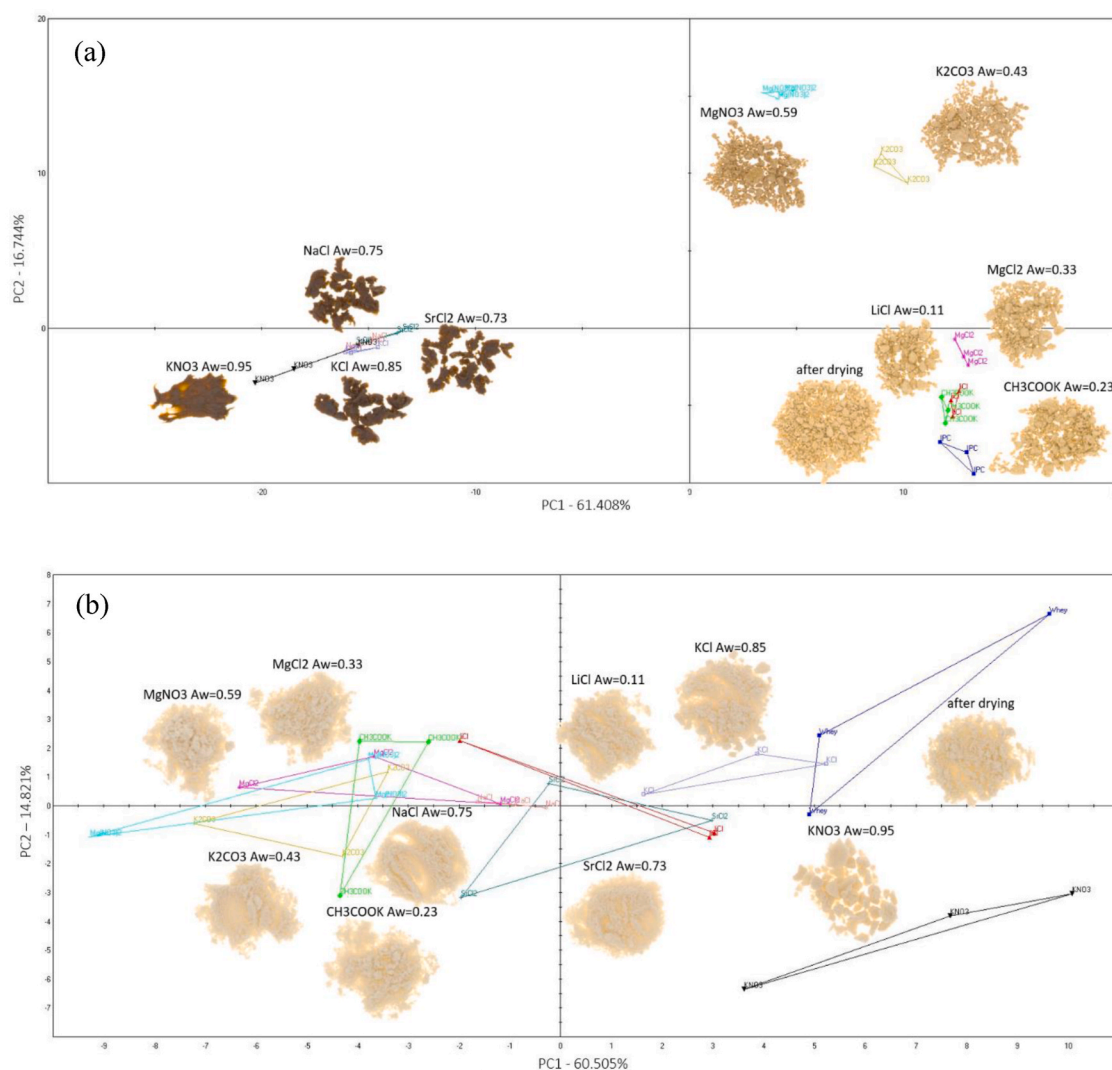


Fig. 4. PCA plots of IPC (a) and WPC (b) at 0.11–0.96 water activity (A_w) range at 20 °C based on Iris color analysis. Photos show IPC and WPC powders and corresponding saturated salt solutions. Lines of the same colors connect the points of a sample at a particular A_w . (For interpretation of the references to color in this figure legend, the reader is referred to the Web version of this article.)

powders are of interest for future studies. Additionally, the porous structure of IPC with a larger surface area could increase the reaction rate (Stoklosa, Lipasek, Taylor, & Mauer, 2012).

3.5. Moisture adsorption isotherms

The adsorption data at 5 and 20 °C are listed in Table S3. The

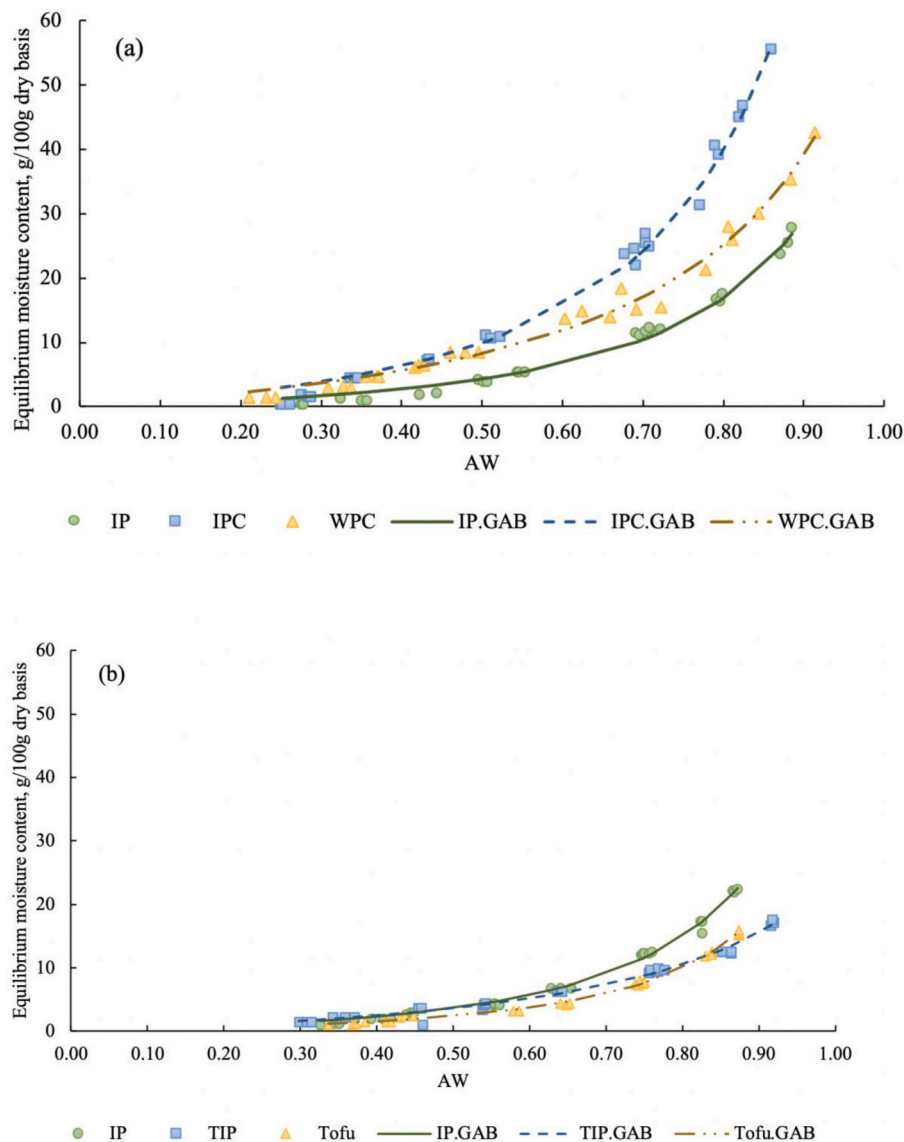


Fig. 5. Moisture adsorption isotherms at 20 °C (a) and 5 °C (b).

isotherms of all samples obtained (Fig. 5) were type III according to Brunauer classification (Brunauer, 2007). Isotherms of this type are relatively rare but frequently found in products containing high carbohydrate content (Blahovec & Yanniotis, 2009). The use of pre-drying method or the properties of products resulted in the lack of data points at water activities below 0.1, which could influence the determination of isotherm shape. It was also found in pineapple pulp powder that some moisture remained after drying, which led to a lack of data points below A_w of 0.1 (Viganó et al., 2012). Therefore, optimization of pre-drying method is needed to determine the isotherm shapes at low A_w values.

At 20 °C IPC had the highest equilibrium moisture content at the same water activity value, followed by WPC and IP (Fig. 5a). These three isotherm curves differed significantly as water activity increased. IPC exhibited the strongest water-binding capacity, followed by WPC and IP (Table 2), that suggests that at room temperature, IPC could absorb and bind much more water vapor than WPC and IP. Stoklosa et al. observed that smaller glass beads gained more weight than larger sized particles during water adsorption (Stoklosa et al., 2012). The increased absorption of moisture with decreasing particle size was also reported for crystalline sucrose (Rogé & Mathlouthi, 2000). Besides, Yang et al.

Table 2
Water binding capacity data at 20 °C and 5 °C determined by moisture adsorption isotherm.

A_w	Water binding capacity, g water/100g solids		
0.95	IP 20 °C $25.6 \pm 2.0^{b, 1-2}$	IPC 20 °C 49.0 ± 5.6^a	WPC 20 °C 36.0 ± 6.4^b
0.96	IP 5 °C 22.1 ± 0.3^a	TIP 5 °C 17.1 ± 0.4^b	Tofu 5 °C 15.6 ± 0.4^c

¹ Mean \pm standard deviation, $n = 3$.
² The same superscript letters in the same row are not significantly different ($p > 0.05$).

found that more water was absorbed in the potato chips with a higher percentage of porosity (Yang, Martin, Richardson, & Wu, 2017). Therefore, porous microstructure of IPC might explain its large amount of absorbed water. Also, the changes in texture and composition of IPC due to agglomeration and browning formation could affect its moisture adsorption. Although WPC contains the smallest sized particles, lack of porous structure might result in less amount of absorbed water than that of IPC. As for IP, large particle size and lack of porous structure caused

the least absorption of moisture content.

At 5 °C, the isotherms of IP, TIP, and tofu were similar at lower water activities as shown in Fig. 5b. But IP differed from TIP and tofu in adsorption behavior as water activity increased. At higher water activities ($A_w > 0.60$), the equilibrium moisture content of IP was much higher than that of TIP and tofu at the same A_w value. This could be linked to the different interactions between water molecules and food components in IP, TIP, and tofu (Caballero-Cerón et al., 2015). Besides, IP differed from TIP and tofu in structure, which could also lead to the difference in moisture sorption behavior. No significant difference was found in the isotherms of TIP and tofu, which suggests that these two products share similar moisture adsorption properties and could be explained by their similar surface morphology.

3.6. Effect of temperature on adsorption isotherms

The adsorption isotherms of IP fitted with GAB model at 5 and 20 °C are shown in Fig. 5. At the constant water activity, the equilibrium moisture content (EMC) increased with a higher temperature. This means more water molecules were absorbed and bound by IP when increasing temperature. However, the observed result was contrary to the general theory that increasing temperature would decrease the binding energy between molecules and reduce the number of active sites for water adsorption, thus leading to an increase of water activity due to activated water molecules (Caballero-Cerón et al., 2015). Kamau et al. observed a significant decrease of adsorption for cricket and black soldier fly larvae powder with increasing temperature, which was more evident in black soldier fly larvae (Kamau et al., 2018). Vivanco and Taboada also found a decrease in moisture content of fish meal with increasing temperature (Vivanco & Taboada, 1998). This general temperature effect on moisture sorption was also found in many other food products, for instance, sprayed dried tomato pulp (Goula, Karapantsios, Achilias, & Adamopoulos, 2008), sesame flour (Menkov & Durakova, 2007), and macadamia nuts (Palipane & Driscoll, 1993). However, Saravacos and Stinchfield observed an increase in the amount of water absorbed by freeze-dried starch-glucose gel and peach as the temperature rose from -20 to 30 °C (Saravacos & Stinchfield, 1965). Similar behavior was also found on sorption isotherms of raisins (Saravacos, Tsiourvas, & Tsami, 1986), suggesting that the increase of sugar dissolution at higher temperature became the determining factor, which reduced the opposite effect of temperature on the sorption of non-sugar solids (Saravacos et al., 1986).

3.7. Modelling

Seven sorption models were fitted to experimental data. The estimated parameters of models and results of Akaike information criterion are listed in Table S4. The minimum AIC_c value indicates the best quality of fitting. As shown in the table, the GAB model obtained the lowest AIC_c value of all seven models. The adsorption isotherms fitted with GAB model and corresponding residual plots were calculated. GAB model well described the isotherms of all 5 samples at corresponding temperatures, although it overestimated the adsorption data at lower water activities ($A_w < 0.50$), for instance IP at 20 and 5 °C, IPC at 20 °C (Fig. 5). Further evaluation of the goodness of fit was done by analyzing the residual plots and the parameter correlation matrices and uncertainties, this analysis also indicated that the GAB model is appropriate for the data. Considering all factors, the GAB model well described the adsorption isotherms and provided the best fit of all. The Caurie and Oswin models described experimental data reasonably well (figures were not shown), however the ΔAIC_c values of Caurie and Oswin were both higher than 10, indicating that these two models failed to explain some substantial explainable variation in the data (Burnham & Anderson, 2002). Thus, Caurie and Oswin were excluded from further consideration in this case.

3.8. Uncertainties

The uncertainties (U , u_A , u_B) of IP at each water activity condition are listed in Table S5. It has been assumed that all experimental data were normally distributed, although some data were not according to Shapiro-Wilk test, that could be explained by the small sample size. The uncertainties were relatively low, except for the ones at higher water activities. For instance, the U values of IPC and WPC at 20 °C were about 6.48 and 7.27, respectively, at the highest water activity ($A_w = 0.95$, KNO_3). It was also observed that the u_A value generally determined the extended uncertainty U , as the systematic uncertainty u_B was much lower (Table S5). This result was comparable to the evaluation of uncertainties on moisture content of barley straw (Bui et al., 2017).

3.9. Applications

The moisture sorption isotherms are frequently used to predict the stability of food systems. Labuza created a “stability map” describing various physiochemical and biological reactions that could occur in food systems as a function of water activity (Labuza, 1977). Information related to these reactions, such as the rate and occurrence water activity range could be gained from this map. The observation in our study that browning of IPC occurs at $A_w > 0.73$ that is in agreement with the fact, that the non-enzymatic browning could occur above 0.20 water activity (Labuza, 1977). Thus, it is possible to correlate and predict undesirable reactions in lesser mealworm ingredients based on the moisture adsorption isotherms. Besides, Tonon et al. combined the glass transition temperatures with water sorption isotherms and determined the critical water activity and glass transition temperature for food storage (Tonon et al., 2009). Therefore, the isotherms could also be used for preventing undesirable structural or texture changes in food products. Labuza and Altunakar also proposed a model to predict the shelf life of food products (Labuza & Altunakar, 2007). The model calculated parameters can be used to estimate the products shelf life by considering initial and equilibrium moisture content, critical moisture content together with packaging material parameters (permeability, thickness, water vapor transmission rate). In general, packaging of dry powdery and tofu-like insect-derived food ingredients should meet the requirements for limiting the water vapor, oxygen, and light transmission. Based on the results presented concrete shelf life extending measures with regard to agglomeration and browning can be taken by measures that keep a_w below 0.73.

4. Conclusions

IP, IPC, TIP, WPC, and tofu exhibited type III adsorption moisture isotherms according to Brunauer classification in this work. The GAB model best described the data in all isotherms in comparison to other models based on its minimum value of the Akaike information criterion. The random residual distributions of GAB model also proved that the experimental data fitted well to GAB model. IPC absorbed the largest quantity of water at 20 °C probably due to its smaller particle size and porous structure, followed by WPC and IP. TIP and tofu exhibited similar moisture adsorption properties at 5 °C. Evident browning and texture changes were only found in IPC at higher water activities, that could be explained by high carbohydrate content and porous structure. To gain more information about storage conditions or to predict shelf life, more research should be performed and combined with moisture sorption isotherm results, for instance the studies on microbial growth, physical changes or consumer sensory test during storage.

CRedit authorship contribution statement

He Sun: Investigation, Formal analysis, Writing - original draft, Writing - review & editing, Visualization. **Ornella Necoechea Velazco:** Conceptualization, Writing - review & editing, Supervision. **Catriona**

Lakemond: Methodology, Writing - review & editing. **Matthijs Dekker:** Methodology, Validation, Writing - review & editing. **Lee Cadesky:** Conceptualization, Writing - review & editing. **Maryia Mishyna:** Conceptualization, Writing - review & editing, Supervision.

Declaration of competing interest

There is no competing conflict among all authors.

Acknowledgements

The author would like to thank Wageningen Electron Microscopy Centre for the scanning electron microscopy analysis.

Appendix A. Supplementary data

Supplementary data to this article can be found online at <https://doi.org/10.1016/j.lwt.2021.110989>.

References

- Aguilera, J. M., del Valle, J. M., & Karel, M. (1995). Caking phenomena in amorphous food powders. *Trends in Food Science & Technology*, 6(5), 149–155. [https://doi.org/10.1016/S0924-2244\(00\)89023-8](https://doi.org/10.1016/S0924-2244(00)89023-8)
- Al-Muhtaseb, A. H., McMinn, W. A. M., & Magee, T. R. A. (2002). Moisture sorption isotherm characteristics of food products: A review. *Food and Bioprocess Technology*, 80(2), 118–128. <https://doi.org/10.1205/09603080252938753>
- Azzollini, D., Derossi, A., & Severini, C. (2016). Understanding the drying kinetic and hygroscopic behaviour of larvae of yellow mealworm (*Tenebrio molitor*) and the effects on their quality. *Journal of Insects as Food and Feed*, 2(4), 233–243. <https://doi.org/10.3920/JIFF2016.0001>
- Bell, S. (2001). *A beginner's guide to uncertainty of measurement*. Teddington, Middlesex, United Kingdom.
- Blahovec, J., & Yanniotis, S. (2009). Modified classification of sorption isotherms. *Journal of Food Engineering*, 91(1), 72–77. <https://doi.org/10.1016/j.jfoodeng.2008.08.007>
- van Broekhoven, S., Oonincx, D. G. A. B., van Huis, A., & van Loon, J. J. A. (2015). Drying performance and feed conversion efficiency of three edible mealworm species (Coleoptera: Tenebrionidae) on diets composed of organic by-products. *Journal of Insect Physiology*, 73, 1–10. <https://doi.org/10.1016/j.jinsphys.2014.12.005>
- Brunauer, S. (2007). *The adsorption of gases and vapors vol I - physical adsorption* (Vol. 1). Brunauer Press.
- Buera, M., Lozano, R., & Petriella, C. (1986). Definition of color in the non-enzymatic browning process. *Farbe*, 32, 318–322.
- Bui, R., Labat, M., & Aubert, J.-E. (2017). Comparison of the saturated salt solution and the dynamic vapor sorption techniques based on the measured sorption isotherm of barley straw. *Construction and Building Materials*, 141, 140–151. <https://doi.org/10.1016/j.conbuildmat.2017.03.005>
- Burnham, K. P., & Anderson, D. R. (2002). *Model selection and multimodel inference. A practical information-theoretic approach*. New York: Springer-Verlag.
- Caballero-Cerón, C., Guerrero-Beltrán, J. A., Mújica-Paz, H., Torres, J. A., & Welti-Chanes, J. (2015). Moisture sorption isotherms of foods: Experimental methodology, mathematical analysis, and practical applications. In *Water stress in biological, chemical, pharmaceutical and food systems* (pp. 187–214). New York: Springer. https://doi.org/10.1007/978-1-4939-2578-0_15
- Caurie, M. (1981). Derivation of full range moisture sorption isotherms. In L. B. Rockland, & G. F. Stewart (Eds.), *Water activity: Influences on food quality. A treatise on the influence of bound and free water on the quality and stability of foods and other natural products* (pp. 63–87). New York: Academic Press.
- Chen, J. Y., Piva, M., & Labuza, T. P. (1984). Evaluation of water binding capacity (WBC) of food fiber sources. *Journal of Food Science*, 49, 59–63. <https://doi.org/10.1111/j.1365-2621.1984.tb13668.x>
- DeFoliart, G. R. (1992). Insects as human food. Gene DeFoliart discusses some nutritional and economic aspects. *Crop Protection*, 11(5), 395–399. [https://doi.org/10.1016/0261-2194\(92\)90020-6](https://doi.org/10.1016/0261-2194(92)90020-6)
- Fasolin, L. H., Pereira, R. N., Pinheiro, A. C., Martins, J. T., Andrade, C. C. P., Ramos, O. L., et al. (2019). Emergent food proteins - towards sustainability, health and innovation. *Food Research International*, 125, 108586. <https://doi.org/10.1016/j.foodres.2019.108586>. Elsevier Ltd.
- Goula, A. M., Karapantsios, T. D., Achilias, D. S., & Adamopoulos, K. G. (2008). Water sorption isotherms and glass transition temperature of spray dried tomato pulp. *Journal of Food Engineering*, 85(1), 73–83. <https://doi.org/10.1016/j.jfoodeng.2007.07.015>
- Greenspan, L. (1977). Humidity fixed points of binary saturated aqueous solutions. *Journal of Research of the National Bureau of Standards*, 81(1), 89–96.
- Guerrero, S., Alzamora, S. M., & Gerschenson, L. N. (1996). Optimization of a combined factors technology for preserving banana purée to minimize colour changes using the response surface methodology. *Journal of Food Engineering*, 28(3-4), 307–322. [https://doi.org/10.1016/0260-8774\(95\)00036-4](https://doi.org/10.1016/0260-8774(95)00036-4)
- Horwitz, W. (1975). *Official methods of analysis*. Washington, DC: Association of Official Analytical Chemists.
- van Huis, A., & Tomberlin, J. K. (Eds.). (2017). *Insects as food and feed: From production to consumption*. The Netherlands: Wageningen Academic Publishers. <https://doi.org/10.3920/978-90-8686-849-0>
- Janssen, R. H., Vincken, J. P., Van Den Broek, L. A. M., Fogliano, V., & Lakemond, C. M. M. (2017). Nitrogen-to-protein conversion factors for three edible insects: *Tenebrio molitor*, *Alphitobius diaperinus* and *Hermetia illucens*. *Journal of Agricultural and Food Chemistry*, 65, 2275–2278. <https://doi.org/10.1021/acs.jafc.7b00471>
- Kamau, E., Mutungi, C., Kinyuru, J., Imathiu, S., Tanga, C., Affognon, H., et al. (2018). Moisture adsorption properties and shelf-life estimation of dried and pulverised edible house cricket *Acheta domesticus* (L.) and black soldier fly larvae *Hermetia illucens* (L.). *Food Research International*, 106, 420–427. <https://doi.org/10.1016/j.FOODRES.2018.01.012>
- Kassambara, A. (2016). *Practical guide to principal component methods in R*. Khatib, K. A., Aramouni, F. M., Herald, T. J., & Boyer, J. E. (2002). Physicochemical characteristics of soft tofu formulated from selected soybean varieties. *Journal of Food Quality*, 25, 289–303. <https://doi.org/10.1111/j.1745-4557.2002.tb01026.x>
- Kiranoudis, C. T., Maroulis, Z. B., Tsami, E., & Marinou-Kouris, D. (1993). Equilibrium moisture content and heat of desorption of some vegetables. *Journal of Food Engineering*, 20, 55–74. [https://doi.org/10.1016/0260-8774\(93\)90019-G](https://doi.org/10.1016/0260-8774(93)90019-G)
- Labuza, T. P. (1977). The properties of water in relationship to water binding in foods: A review. *Journal of Food Processing and Preservation*, 1, 167–190.
- Labuza, T. P., & Altunakar, L. (2007). Water activity prediction and moisture sorption isotherms. In G. V. Barbosa-Cánovas, A. J. Fontana Jr, S. J. Schmidt, & T. P. Labuza (Eds.), *Water activity in foods: Fundamentals and applications* (pp. 109–154). Oxford, UK: Blackwell Publishing Ltd. <https://doi.org/10.1002/9780470376454.ch5>
- Lenaerts, S., Van Der Borgh, M., Callens, A., & Van Campenhout, L. (2018). Suitability of microwave drying for mealworms (*Tenebrio molitor*) as alternative to freeze drying: Impact on nutritional quality and colour. *Food Chemistry*, 254, 129–136. <https://doi.org/10.1016/j.foodchem.2018.02.006>
- López-Malo, A., Palou, E., & Argaz, A. (1994). Measurement of water activity of saturated salt solutions at various temperatures. In *International symposium on the properties of water* (pp. 113–116).
- Menkov, N. D., & Durakova, A. G. (2007). Moisture sorption isotherms of sesame flour at several temperatures. *Food Technology and Biotechnology*, 45, 96–100.
- Palipane, K. B., & Driscoll, R. H. (1993). Moisture sorption characteristics of in-shell macadamia nuts. *Journal of Food Engineering*, 18(1), 63–76. [https://doi.org/10.1016/0260-8774\(93\)90075-U](https://doi.org/10.1016/0260-8774(93)90075-U)
- Palou, E., Lopez-Malo, A., Barbosa-Canovas, G. V., Welti-Chanes, J., & Swanson, B. G. (1999). Polyphenoloxidase activity and color of blanched and high hydrostatic pressure treated banana puree. *Journal of Food Science*, 64(1), 42–45. <https://doi.org/10.1111/j.1365-2621.1999.tb09857.x>
- Rahman, M. S. (2010). Food stability determination by macro-micro region concept in the state diagram and by defining a critical temperature. *Journal of Food Engineering*, 99(4), 402–416. <https://doi.org/10.1016/j.jfoodeng.2009.07.011>
- Rogé, B., & Mathlouthi, M. (2000). Caking of sucrose crystals: Effect of water content and crystal size. *Zuckerindustrie*, 125(5), 336–340.
- Rouch, D. A., Roupas, P., & Roginski, H. (2007). True protein value of milk and dairy products. *Australian Journal of Dairy Technology*, 62(1), 26–30.
- Salter, C., & De Levie, R. (2002). Nonlinear fits of standard curves: A simple route to uncertainties in unknowns. *Journal of Chemical Education*, 79(2), 268. <https://doi.org/10.1021/ed079p268>
- Saravacos, G., & Stinchfield, R. (1965). Effect of temperature and pressure on the sorption of water vapor by freeze-dried food materials. *Journal of Food Science*, 30, 779–786.
- Saravacos, G., Tsiourvas, D., & Tsami, E. (1986). Effect of temperature on the water adsorption isotherms of sultana raisins. *Journal of Food Science*, 51, 381–383.
- Sawhney, I. K., Sarkar, B. C., Patil, G. R., & Sharma, H. K. (2014). Moisture sorption isotherms and thermodynamic properties of whey protein concentrate powder from buffalo skim milk. *Journal of Food Processing and Preservation*, 38(4), 1787–1798. <https://doi.org/10.1111/jfpp.12148>
- Shockley, M., Allen, R. N., & Gracer, D. (2017). *Product development and promotion. In Insects as food and feed: From production to consumption* (pp. 398–427). Wageningen Academic Publisher.
- Singh, R. R. B., Rao, K. H., Anjaneyulu, A. S. R., & Patil, G. R. (2001). Moisture sorption properties of smoked chicken sausages from spent hen meat. *Food Research International*, 34(2-3), 143–148. [https://doi.org/10.1016/S0963-9969\(00\)00145-9](https://doi.org/10.1016/S0963-9969(00)00145-9)
- Smith, S. E. (1947). The sorption of water vapor by high polymers. *Journal of the American Chemical Society*, 69(3), 646–651. <https://doi.org/10.1021/ja01195a053>
- Stoklosa, A. M., Lipasek, R. A., Taylor, L. S., & Mauer, L. J. (2012). Effects of storage conditions, formulation, and particle size on moisture sorption and flowability of powders: A study of deliquescent ingredient blends. *Food Research International*, 49(2), 783–791. <https://doi.org/10.1016/j.foodres.2012.09.034>
- Strange, E. D., & Onwulata, C. I. (2002). Effect of particle size on the water sorption properties of cereal fibers. *Journal of Food Quality*, 25(1), 63–73. <https://doi.org/10.1111/j.1745-4557.2002.tb01008.x>
- Tham, T. W. Y., Wang, C., Yeoh, A. T. H., & Zhou, W. (2016). Moisture sorption isotherm and caking properties of infant formulas. *Journal of Food Engineering*, 175, 117–126. <https://doi.org/10.1016/j.jfoodeng.2015.12.014>
- Tonon, R. V., Baroni, A. F., Brabet, C., Gibert, O., Pallet, D., & Hubinger, M. D. (2009). Water sorption and glass transition temperature of spray dried açaí (*Euterpe oleracea* Mart.) juice. *Journal of Food Engineering*, 94(3-4), 215–221. <https://doi.org/10.1016/j.jfoodeng.2009.03.009>

- United Nations. (2019). *World population prospects*. Retrieved from <https://population.un.org/wpp/> Accessed April 28, 2020.
- Viganó, J., Azuara, E., Telis, V. R. N., Beristain, C. I., Jiménez, M., & Telis-Romero, J. (2012). Role of enthalpy and entropy in moisture sorption behavior of pineapple pulp powder produced by different drying methods. *Thermochimica Acta*, 528, 63–71. <https://doi.org/10.1016/j.tca.2011.11.011>
- Vivanco, M. M., & Taboada, O. M. (1998). Thermodynamic behavior of fish meal during adsorption. *Drying Technology*, 16(9-10), 1827–1842. <https://doi.org/10.1080/07373939808917498>
- Wallingford, L., & Labuza, T. P. (1983). Evaluation of the water binding properties of food hydrocolloids by physical/chemical methods and in a low fat meat emulsion. *Journal of Food Science*, 48(1), 1–5. <https://doi.org/10.1111/j.1365-2621.1983.tb14775.x>
- Yang, J., Martin, A., Richardson, S., & Wu, C.-H. (2017). Microstructure investigation and its effects on moisture sorption in fried potato chips. *Journal of Food Engineering*, 214, 117–128. <https://doi.org/10.1016/j.jfoodeng.2017.06.034>
- Yi, L., Lakemond, C. M. M., Sagis, L. M. C., Eisner-Schadler, V., van Huis, A., & van Boekel, M. A. J. S. (2013). Extraction and characterisation of protein fractions from five insect species. *Food Chemistry*, 141, 3341–3348. <https://doi.org/10.1016/j.foodchem.2013.05.115>
- Zafar, U., Vivacqua, V., Calvert, G., Ghadiri, M., & Cleaver, J. A. S. (2017). A review of bulk powder caking. *Powder Technology*, 313, 389–401. <https://doi.org/10.1016/j.powtec.2017.02.024>